Journal of Archaeological Science 37 (2010) 3370–3384

Contents lists available at ScienceDirect

Journal of Archaeological Science

journal homepage: http://www.elsevier.com/locate/jas

The 74 ka Toba super-eruption and southern Indian hominins: archaeology, lithic technology and environments at Jwalapuram Locality 3

Michael Haslam [a,*], Chris Clarkson [b], Michael Petraglia [a], Ravi Korisettar [c], Sacha Jones [d], Ceri Shipton [e], Peter Ditchfield [a], Stanley H. Ambrose [f]

[a] *School of Archaeology, Research Laboratory for Archaeology and the History of Art, University of Oxford, Oxford OX1 3QY, United Kingdom*
[b] *School of Social Science, University of Queensland, St Lucia QLD 4072, Australia*
[c] *Department of History and Archaeology, Karnatak University, Dharwad 580 003, India*
[d] *McDonald Institute for Archaeological Research, University of Cambridge, Cambridge CB2 3ER, United Kingdom*
[e] *School of Geography and Environmental Science, Monash University, Melbourne, Victoria 3800, Australia*
[f] *Department of Anthropology, University of Illinois, Urbana, IL 61801, USA*

ARTICLE INFO

Article history:
Received 13 February 2010
Received in revised form
27 May 2010
Accepted 1 July 2010

Keywords:
South Asia
Late Pleistocene
Middle Palaeolithic
Human dispersal
Isotopes
Palaeoenvironment

ABSTRACT

Hominins living in southern India 74,000 years ago faced a deteriorating environment, as the global climate moved from interglacial into full glacial conditions. At the same time, South Asian populations witnessed the widespread deposition of tephra from the Sumatran Toba super-eruption, the largest explosive volcanic event of the past two million years. Here we report new data on the lithic technology and environmental context for a southern Indian site with hominin occupation in association with Toba tephra deposits: Jwalapuram Locality 3 in the Jurreru Valley. Sedimentological and isotopic studies demonstrate that a cooling trend was in effect in this part of southern India prior to the eruption, and that thick deposits of ash in the Jurreru Valley supported grassland communities before more wooded conditions were re-established. Detailed technological analyses of an expanded lithic sample from Locality 3 suggest cultural continuity after the eruptive event, and comparisons with lithic core technologies elsewhere indicate that *Homo sapiens* cannot be ruled out as the creator of these Middle Palaeolithic assemblages.

1. Introduction

Hominin occupation bracketing tephra from the ~74,000 BP Youngest Toba Tuff (YTT) super-eruption was recently reported from southern India (Petraglia et al., 2007). This discovery, from the Jurreru River Valley in Andhra Pradesh, has relevance for discussions of the routes and timing of *Homo sapiens* dispersals out of Africa. Palaeoenvironmental data from this area also assist with the identification of local responses to the potentially abrupt environmental effects of the Toba event. Analysis of lithic core assemblages from the Jurreru Valley, dated close to the time of the eruption, showed closer affinities to African Middle Stone Age traditions than to the contemporaneous Levantine Middle Palaeolithic. The Jurreru occupations also fall close to the early range of proposed out of Africa genetic coalescence (Macaulay et al., 2005; Oppenheimer, 2009). Along with the implication of population continuity of Middle Palaeolithic populations up until 38 ka (Petraglia et al., 2009a, 2009b), these findings raised the possibility that modern humans may have been responsible for creating the Jurreru Valley assemblages.

Here we describe and discuss the excavation, sedimentary sequence and associated lithic assemblage of Jwalapuram Locality 3 in the Jurreru Valley (Fig. 1). This article expands upon earlier reports (Petraglia et al., 2009b, 2007), and includes previously unpublished data from new excavations conducted at the site. We place the findings within broader debates over the development of the Indian Middle Palaeolithic and the impact of the Toba eruption on regional environments.

2. Jwalapuram Locality 3

Jwalapuram Locality 3 (N 15°19′20″ E 78°08′01″) is a volcanic ash quarry approximately 0.5 km west of the village of Jwalapuram and 400 m south of the eastwards-flowing Jurreru River. The hand-excavated quarry covers some 500 m^2 at present, and is one of several in the immediate area that exploit a considerable quantity of relatively pure YTT deposits. The mean tephra thickness across the valley is just over 1 m (Jones, 2007), and the volume of buried

* Corresponding author. Tel.: +44 0 1865 275134; fax: +44 0 1865 285220.
E-mail address: michael.haslam@rlaha.ox.ac.uk (M. Haslam).

0305-4403/$ – see front matter
doi:10.1016/j.jas.2010.07.034

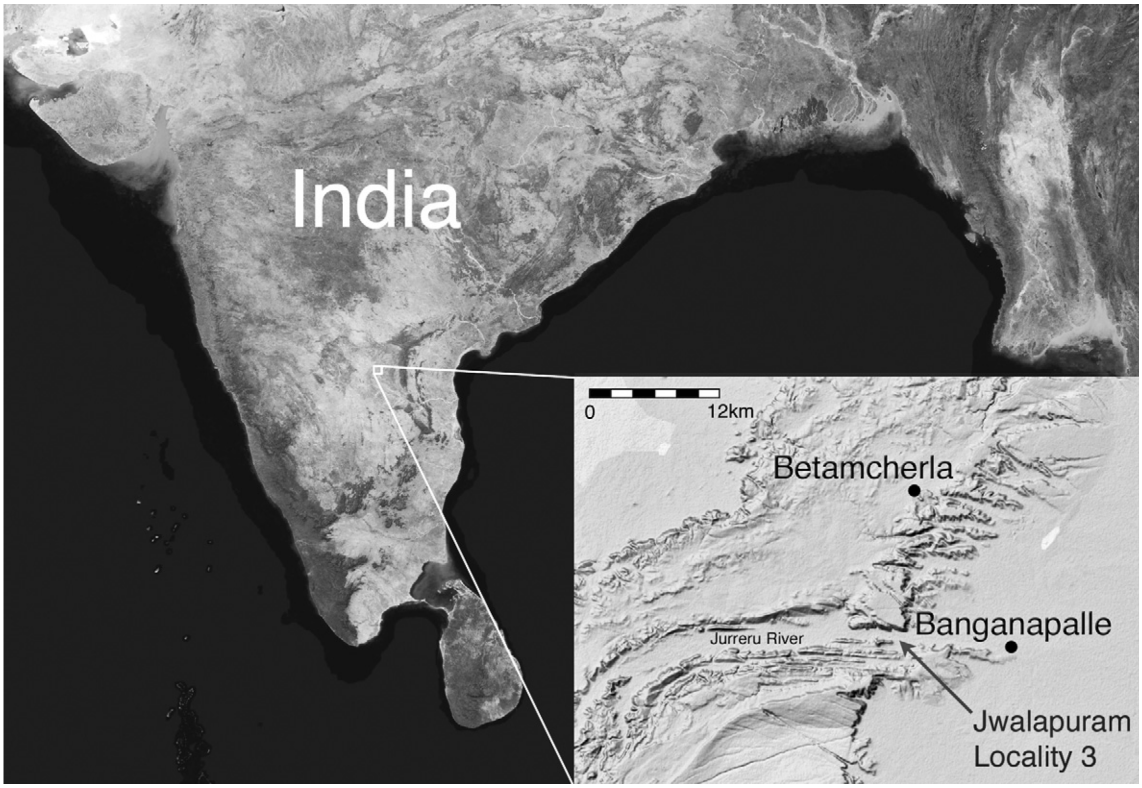

Fig. 1. Location of Jwalapuram Locality 3.

tephra within the immediate area likely exceeds 1 million cubic metres, as recent observations indicate that previous extrapolations from exposed mine sections are likely underestimates. The introduction of mechanised and explosive ash removal has resulted in an accelerating destruction of the upper portion of the landscape. The tephra deposit that runs through the Locality 3 site was briefly reported in the early 1990s by the Geological Survey of India (Rao and Rao, 1992). Following this report, the interdisciplinary Kurnool District Archaeological Project (KDAP) excavated the site between 2003 and 2009 (Petraglia et al., 2009b). The ash has been geochemically identified as YTT (Petraglia et al., 2007) and is ~1.8–2.4 m thick in a continuous layer across the site, forming an unambiguous and reliable isochron. Quarrying activities continue to destroy the site.

The Kurnool District of Andhra Pradesh is classed as semi-arid, with mean annual rainfall of around 850 mm and regular failure of the monsoon. The immediate environmental context is one of sparse dry Acacia scrub and exposed compact red silts pot-holed by numerous small ash-quarries. The Jurreru River dam lies 1 km upstream, and irrigated agricultural fields range to the south of the exposed quarried area. There is abundant evidence for termite activity in the surrounding area in the form of termite mounds and the active breakdown of woody debris. The present-day size of the Jurreru River is insufficient to have formed the wide, flat-bottomed valley that cuts through the Erramala Hills, which suggests past headwater capture or tectonic movement. The extent of preserved tephra indicates that this capture occurred prior to the Toba eruption, and likely much earlier. The local geology is comprised of shales, quartzites and dolomite cherts of the Middle Proterozoic Cuddapah basin, with younger rocks of the Kurnool Supergroup including the Banganapalle and Paniam quartzites predominantly forming the valley sides (Petraglia et al., 2009b; Prasad, 1996). These quartzites have weathered into a series of large rockshelters along the northern flank of the valley that preserve the earliest known microlithic assemblage in India (Clarkson et al., 2009; Petraglia et al., 2009a). The highly siliceous Narji limestone has produced a series of dissolution caves to the north of the Jurreru Valley (Haslam et al., 2010), and this material is mined extensively in the local area for tiles. In combination the local limestone and quartzite formations provided an excellent source of lithic raw materials. Long-term occupation of the valley is indicated by lithic and ceramic artefacts from both stratified and surface contexts that have been classified technologically as ranging from the Acheulean through the Middle Palaeolithic, Microlithic, Neolithic and Iron Age to modern times.

Four areas were excavated at Jwalapuram Locality 3 between 2003 and 2009. These include excavations both below (Trenches 3 and 3A) and above (Trenches 3B and 23) the tephra layer, as well as one excavation through both the overlying sediments and the ash itself (Trench 3). All excavated areas are located within an area of approximately 20 × 30 m in undisturbed sediments on the margins of the quarried area, as considerable mining talus obscures much of the locality. Lithic artefacts were recovered from all excavated trenches, although no artefacts have yet been recovered from within the ash bed. Table 1 describes the six major sedimentary units (Strata A–F from the top downwards) at Locality 3 and their correlation with the excavated trenches.

2.1. Excavations above and through the YTT deposits

Three trenches (3, 3B and 23) targeted the sediments overlying the YTT deposits at Locality 3 (Fig. 2). Each was excavated in 5 cm levels and dry-sieved through 5 mm mesh screens. Care was taken to ensure excavated levels did not cross stratigraphic boundaries, to permit accurate assignation of finds to strata. An area totalling 33.5 m^2 was opened up, including 5.5 m^2 at Trench 3, 3 m^2 at

Table 1
Correlation of strata, sedimentary phases and excavated trenches at Jwalapuram Locality 3.

Str.	Phase	Description	Trenches
A	6	Orange sandy gravels with a silty sand matrix	3, 23, 3B
B	5	Orange pedogenically altered ash-rich silty sand	3, 23, 3B
C	4	Light grey reworked volcanic ash with a thin (~4 cm) basal primary ash layer and six fining-upwards beds separated by prominent and laterally extensive hard bands. The upper part of each bed shows evidence of microbial mat formation, ripple structures and desiccation cracking. The base of this unit shows soft-sediment deformation structures.	3
D	3	Orange pedogenically altered lacustrine/palludal clay	3, 3A
E	2	Locally-channelised, clast supported angular pebble conglomerate with red silty matrix	3, 3A
F	1	Orange to grey pedogenically altered silty clay	3, 3A

Trench 3B and 25 m^2 at Trench 23. Trench 3B only removed stratum A deposits, while the other two excavations included strata A and B as well as part (Trench 23) or all (Trench 3) of the YTT layer (stratum C). Samples of soil carbonate nodules and rhizoliths (calicified root casts) were collected from all trenches for isotopic and morphological analysis, and comprehensive sampling was conducted for palaeoenvironmental and sedimentological analysis, the results of which are discussed below.

Excavation through the Toba tephra layer at Locality 3 revealed that it was divided by thin, grey, fine-grained, near-horizontal hardpan layers into six beds of varying thickness. The ash beds were remarkable for the apparent lack of significant observable extraneous sediment, however they did contain frequent fossilised and unfossilised roots, fossilised termite nests, and minor clay and sand components. Large quantities of similar fossilised material

Fig. 2. Excavations in progress at Jwalapuram Locality 3, with strata indicated: (a) Trench 3, above and below the YTT. Note that the darker lower section of the ash profile (Stratum C) is caused by ephemeral differential water retention; (b) Trench 3, through the YTT revealing bedding of ash layers; (c) Trench 3B, above the YTT; (d) Trench 23, above the YTT (scales are both 50 cm).

litter the quarry sites in the valley, as it is considered waste material by the local ash miners. Fossilised material reached a maximum of around 37 kg/m^3 in the middle of the YTT deposit, with values for the other ash beds between approximately 10 and 25 kg/m^3 (Jones, 2007). Both modern and fossilised rootlets penetrate the hardpan layers in places, however these result in only very minor intermixing of material between the different beds. The ash beds also retain some evidence of fine undulations within their structure, and at other sites in the Jurreru Valley there is evidence of trees being encased in the thick ash deposits, indicating that deposition was not always into still water environments. It is likely that the large tephra volume entering the Jurreru Valley contributed to choking of the Jurreru River, which in turn increased the likelihood of standing, shallow overbank waters either side of the river channel.

2.2. Excavations below the YTT deposits

Two trenches (3 and 3A) were excavated downwards from the exposed floor of the Locality 3 quarry (Fig. 3), which marks the initial deposition of Toba ash in the Jurreru Valley and therefore dates to the time of the YTT eruption at ~74 ka (Oppenheimer, 2002; Westgate et al., 1998). The below-ash Trench 3 was a test excavation covering an area of 1.5 m^2, which was rapidly excavated in 10 cm levels to a depth of 2 m below the YTT interface without encountering cultural material, at which point the local water table was encountered. Trench 3A was also excavated in 10 cm levels and dry-sieved through 5 mm mesh, revealing an implementiferous stratum approximately 1.2 m below the Toba tephra (see below). This latter trench has provided all of the stratigraphically secure artefacts from pre-Toba contexts at Jwalapuram Locality 3. Trench 3A was initially excavated across a 9 m^2 area to provide the previously reported lithic data (Petraglia et al., 2007), with subsequent expansion to 24.75 m^2 to facilitate greater artefact recovery. The maximum depth reached in Trench 3A was 3.7 m below the base of the YTT deposit, however excavations were only continued beneath the artefact-bearing stratum in 2.5 m^2 in the southeast of the excavated area.

3. Sedimentary and palaeoenvironmental sequence

3.1. Materials and methods

To assess the environmental and formation processes active during sedimentation at Locality 3, particle size, magnetic susceptibility, organic loss on ignition and percentage carbonate data were obtained for the site profile. Samples analysed by these methods span the interval between strata A and E, including the YTT beds, and further details and methods for these analyses are provided by Jones (2010). In addition, a limited study of phytoliths from the strata above the ash was conducted to assess the potential for preservation and recovery of plant microfossils conducive to palaeoenvironmental reconstruction (Eksambekar, 2008). Stable carbon and oxygen isotopes of carbonate nodules and rhizoliths were analysed primarily from below and within the YTT ash at the site (Table 2). Carbonate samples analysed at the University of Illinois comprise one or two nodules or rhizoliths from over 25 levels throughout the sequence. Those analysed at Oxford University comprise five nodules per level, from five levels below, within and above the YTT ash. The former sampling strategy provides higher resolution on diachronic change; the latter reflects the range of semi-synchronic isotopic variability.

Carbonate nodules processed at Oxford were rinsed in deionised water and treated in an ultrasonic bath for 3 min to remove adhering sediment. Only micritic (fine-grained) pedogenic carbonate nodules were selected for analysis, and those with visible

Fig. 3. Excavation in progress at Jwalapuram Locality 3, with strata indicated: Trench 3A, below the YTT deposits, facing south. This trench was subsequently expanded to the south and west.

Table 2
Stable carbon and oxygen isotope data, Jwalapuram Locality 3.

Sample code[a]	Trench	Stratum	Depth[b]	$\delta^{13}C$‰pdb	$\delta^{18}O$‰ pdb
JWP-3A-152-A	3A	F	−285.0	−7.00	−2.95
JWP-3A-152-B	3A	F	−285.0	−7.36	−4.04
JWP-3A-143	3A	F	−267.0	−6.51	−2.67
JWP-3A-142-A	3A	F	−265.0	−6.40	−2.69
JWP-3A-142-B	3A	F	−265.0	−8.37	−4.72
JWP-3A-141-A	3A	F	−263.0	−6.86	−2.70
JWP-3A-141-B	3A	F	−263.0	−7.91	−4.08
JWP-3A-134-A	3A	F	−249.0	−7.14	−2.90
JWP-3A-134-B	3A	F	−249.0	−6.96	−2.20
JWP-3A-127	3A	F	−235.0	−6.82	−2.50
JWP-3A-123-A	3A	F	−227.0	−6.70	−2.06
JWP-3A-122-A	3A	F	−225.0	−6.69	−3.04
JWP-3A-122-B	3A	F	−225.0	−6.67	−2.63
JWP-3A-108	3A	F	−197.0	−5.81	−1.19
JWP-3A-107	3A	F	−195.0	−6.62	−2.12
JWP-3A-100-A	3A	F	−181.0	−6.40	−1.66
JWP-3A-99	3A	F	−179.0	−6.66	−2.74
JWP-3-39-09-SCJ-A	3A	E	−130.0	−5.51	−1.29
JWP-3-39-09-SCJ-B	3A	E	−130.0	−6.66	−2.16
JWP-3-39-10-SCJ-A	3A	D	−70.0	−5.13	−1.14
JWP-3-01S-SCJ-A	3	D	−10.0	−4.27	−0.72
JWP-3-01S-SCJ-B	3	D	−10.0	−4.59	−1.00
JWP-3-U4-STR.O-L6-A	3	C (YTT)	20.0	−7.14	−2.15
JWP-3-U4-STR.O-L6-B	3	C (YTT)	20.0	−5.21	−1.34
JWP-3-U3-STR.0-L2-A	3	C (YTT)	65.0	−8.43	−4.11
JWP-3-U3-STR.0-L2-B	3	C (YTT)	65.0	−3.94	−1.31
JLP-3-11C-SCJ	3	C (YTT)	100	−7.11	−2.73
JWP-3-U3-STR.L–L4	3	C (YTT)	107.5	−4.71	−1.68
JWP-3-U3&4-STR.N	3	C (YTT)	107.5	−4.15	−1.12
JWP-3-U3-STR.L–L1-A	3	C (YTT)	145.0	−2.80	−1.69
JWP-3-U3-STR.L–L1-B	3	C (YTT)	145.0	−4.05	−2.34
JWP-3-U3-STR.H-A	3	C (YTT)	190.0	−3.47	−1.54
JWP-3-U3-STR.H-B	3	C (YTT)	190.0	−3.81	−0.51
JWP-3-E04-SCJ	3	C (YTT)	200.0	−1.12	−1.48
JWP-3-U4-STR.F-L1-A	3	C (YTT)	205.0	−1.04	−1.62
JWP-3-U4-STR.F-L1-B	3	C (YTT)	205.0	−4.04	−1.31
JWP-3-U3-STR.D-L2	3	C (YTT)	217.5	−2.76	−1.80
JWP-3-U4-STR.D-L1-A	3	C (YTT)	235.0	−3.61	−1.57
JWP-3-U4-STR.D-L1-B	3	C (YTT)	235.0	−4.27	−0.85
JWP-3-E01-SCJ	3	B	240.0	−6.75	−2.46
JWP-3-14S-SCJ	3	B	250.0	−7.05	−2.47
JWP-3-155-SCJ	3	B	290.0	−4.09	−1.93
92607-1	3A	F	−220.0	−5.22	−1.80
92607-2	3A	F	−220.0	−7.05	−1.10
92607-3	3A	F	−220.0	−4.19	−1.60
92607-4	3A	F	−220.0	−7.61	−1.30
92607-5	3A	F	−220.0	−8.23	−1.40
92707-1	3A	D	−70.0	−4.87	−2.56
92707-2	3A	D	−70.0	−5.01	−2.81
92707-3	3A	D	−70.0	−6.24	−3.55
92707-4	3A	D	−70.0	−5.97	−1.92
92707-5	3A	D	−70.0	−4.41	−2.70
92708-1	3	C (YTT)	40.0	−5.65	−2.30
92708-2	3	C (YTT)	40.0	−5.38	−1.40
92708-3	3	C (YTT)	40.0	−5.20	−2.70
92708-4	3	C (YTT)	40.0	−4.90	−2.14
92708-5	3	C (YTT)	40.0	−6.01	−2.67
92709-1	3	C (YTT)	160.0	−4.85	−2.00
92709-2	3	C (YTT)	160.0	−4.89	−2.40
92709-3	3	C (YTT)	160.0	−5.19	−1.80
92709-4	3	C (YTT)	160.0	−4.93	−3.44
92709-5	3	C (YTT)	160.0	−5.22	−2.43
92710-1	3	B	280.0	−6.79	−2.70
92710-2	3	B	280.0	−7.07	−3.80
92710-3	3	B	280.0	−7.53	−2.80
92710-4	3	B	280.0	−8.18	−3.60
92710-5	3	B	280.0	−9.64	−3.70

[a] Sample codes starting with JWP or JLP were processed at the University of Illinois Environmental Isotope Paleobiogeochemistry Laboratory. All others were processed at the Research Laboratory for Archaeology and the History of Art, University of Oxford.

[b] Negative values represent depths below the base of the YTT deposit. Positive values fall within and overlying the YTT deposit.

sparry (macro-crystalline) carbonate cements were rejected, as they were likely to have been diagenetically altered. Nodules were dried in a 60 °C oven then crushed in an agate pestle and mortar. Oxygen and carbon stable isotopic results were obtained using a VG Isogas Prism II mass spectrometer with an on-line VG Isocarb common acid bath preparation system. Each sample was reacted with purified phosphoric acid (H_3PO_4) at 90 °C with the liberated carbon dioxide cryogenically distilled prior to admission to the mass spectrometer. Both oxygen and carbon isotopic ratios are reported relative to the VPDB international standard. Calibration was against the in-house NOCZ Carrara Marble standard with a reproducibility of better than 0.2‰.

Carbonates processed in the University of Illinois Environmental Isotope Paleobiogeochemistry Laboratory were selected among specimens that exceeded a minimum thickness of 4 mm in order to avoid contamination from softer weathered surface rinds. The mean and standard deviation of length width and thickness of analysed specimens is 50.8 ± 17.2, 16.5 ± 7.4, and 11.7 ± 4.5 mm, respectively. Specimens were split with a stainless steel bar and anvil, and fractured cross-section faces were inspected to identify coarse recrystallized calcite and voids with secondary sparry calcite. Dense micritic cores of samples were drilled with a spherical diamond burr in a mini-drill at the lowest speed setting, slowed further by reducing line voltage 20–25%, in order to avoid overheating. Drilled powder samples weighing 38.3 ± 8.8 mg were placed in 9 mm borosilicate culture tubes and roasted under vacuum at 400 °C for 4 h to reduce organic carbon and remove water and weakly-bound hydroxyls. Weight loss averaged 2.06 ± 0.96%. Samples weighing 57 ± 9 μg were reacted with 100% phosphoric acid at 70 °C in a Kiel III automated cryogenic distillation device coupled to a MAT252 mass spectrometer. National Institutes of Science and Technology (USA) carbonate standards NBS18 or NBS19 were run after every seventh sample. Precision is ±0.06‰ for carbon and ±0.10‰ for oxygen. Stable isotope ratios are expressed using the δ notation as difference in parts per thousand (permil, ‰) relative to the PDB standard, calculated as $\delta‰ = ((R_{sample}/R_{standard}) - 1) \times 1000$, where $R = {}^{13}C/{}^{12}C$ or ${}^{18}O/{}^{16}O$.

The carbon isotope ratio of pedogenic carbonate reflects that of the floral biomass, with an enrichment of 14–17‰ (Cerling, 1999). Proportions of woody (C_3) to tropical grass (C_4) plant biomass are calculated assuming the average $\delta^{13}C$ values of dry tropical forest plants and tropical grasses are −26.5‰ and −12.5‰, respectively, with an average enrichment of +15.5‰. Pedogenic carbonates formed under C_3 forests have $\delta^{13}C$ values of −12‰ to −9‰, while $\delta^{13}C$ values of those formed under C_4 grasslands range from −1‰ to +2‰. Levin et al. (2004), Williams et al. (2009) and WoldeGabriel et al. (2009) provide detailed explanation of environmental interpretation of tropical soil carbonate stable isotope ratios.

3.2. Results

A composite sedimentary log for Locality 3 is presented in Fig. 4, which also indicates the position of optically stimulated luminescence (OSL) samples taken from above and below the YTT deposits. Details of the optical dating procedures are provided elsewhere (Petraglia et al., 2007: SOM). Fig. 5 presents the results of the particle size, magnetic susceptibility, organic loss on ignition and percentage carbonate analyses, while Fig. 6 and Table 2 present the results of soil carbonate stable isotope analyses.

The sedimentary sequence has been divided into six phases corresponding to the six main strata recorded at the site, and the following descriptions build-upon previous research in the Jurreru Valley (Jones, 2007, 2010; Petraglia et al., 2007) (Table 1). The earliest sedimentary phase (Phase 1, Stratum F) revealed by the Locality 3 excavations is one of pedogenically altered calcrete-rich

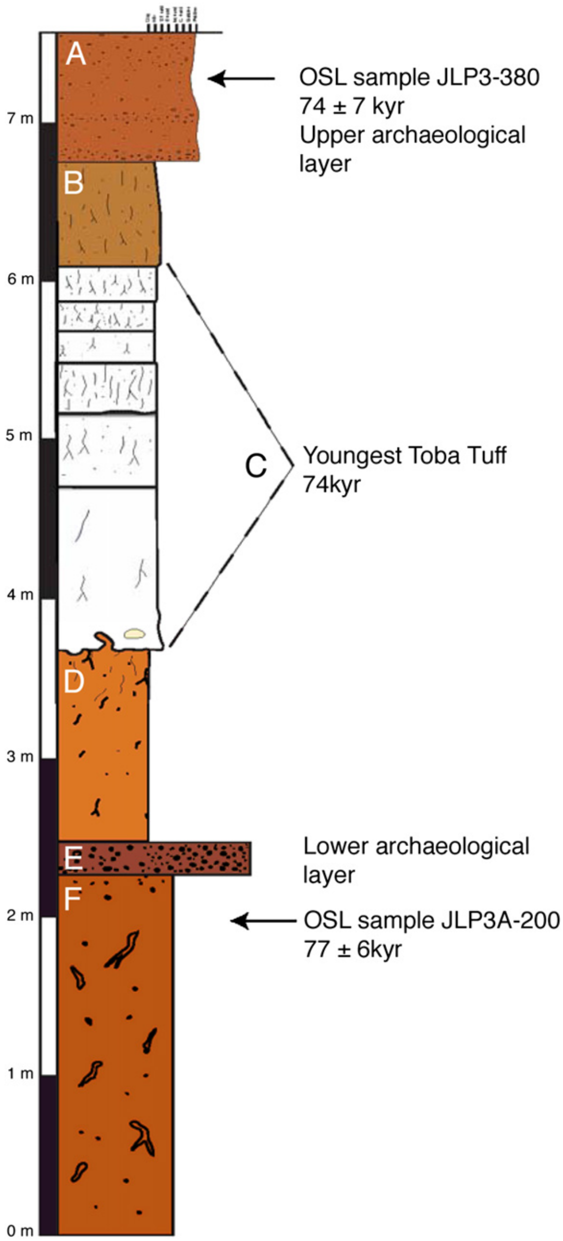

Fig. 4. Composite stratigraphy for Jwalapuram Locality 3, after Petraglia et al. (2007: Figure S2). For strata descriptions see Table 1.

silty greyish clays, suggesting a seasonally wet and perhaps periodically inundated landscape. This may result from a stronger southwest monsoon during the warm Oxygen Isotope Stage (OIS) 5a, as the upper portion of this phase produced an age of 77 ± 6 ka (JLP3A-200).

Stable carbon isotope data from Phase 1 carbonates indicate a mixed C_3/C_4 environment, likely representing grassy woodlands marginal to the central riverine and paludal corridor (Fig. 6). Comparison with East African analogues (Levin et al., 2004; Sikes et al., 1999), and calculations of percent C_4 grass biomass suggests that C_4 terrestrial plants may have made up around 30% of the landscape during Phase 1. Unfortunately faunal preservation in open sites in the Jurreru Valley is exceedingly rare, so corroborating faunal environmental proxies are unavailable. No artefacts were recovered from this phase at Locality 3, suggesting that either the valley was unoccupied or hominin habitation may have been closer to the valley margins at this time. The maximum thickness of the Phase 1 sediments is unknown, but exceeds 2.2 m.

The second depositional phase at Locality 3 (Phase 2, Stratum E) is marked by a channel-derived angular pebble conglomerate, with Middle Palaeolithic artefacts throughout. This layer has a variable thickness of ~25–30 cm. The contact between these sediments and the underlying silty clays is distinct but undulating, indicating that initial inwash of the gravels may have slightly truncated the Phase 1 sediments. Analyses indicate lower magnetic susceptibility and higher calcium carbonate percentages than the overlying Phase 3 sediments, however data on these proxies are not available for the underlying Phase 1. The pebbles and accompanying naturally-occurring ochre pieces in Stratum E are derived from shales found in the medial Kuppakonda hill approximately 1.5 km to the west, suggesting deposition via sheetwash or rills, perhaps with input from braided channels that developed as the margins of the more permanently inundated area of the valley floor contracted. Artefacts from this layer are generally of fresh appearance, with limited instances of abrasion and edge rounding that demonstrate low-energy or short-distance clast transport (Jones, 2010). Stable carbon data indicate that the trend towards more open C_4 environments that was underway at the end of Phase 1 continued in a fairly linear fashion through Phases 2 and 3, with an overall increase in ^{13}C over this period of more than 2‰. Average proportions of C_4 plants increased to 34–47% at 70 cm below the YTT deposits. By the end of Phase 3 (Stratum D), immediately prior to the YTT event, grasslands may have constituted nearly 50% of the local landscape.

Phase 3 deposition at Jwalapuram Locality 3 records the development of approximately 1.2 m of floodplain to lacustrine clays, with occasional localised influx of coarser sediment including manganese-rich gravels. The assessment of wetland development is strengthened by low carbonate levels, decreasing magnetic susceptibility indicative of reduced pedogenesis higher in the profile, and the observation that the overlying YTT preserves soft-sediment deformation structures at the contact between the two strata. An absence of distinct laminations and the presence of preserved rhizoliths and occasional tephra-filled burrows indicate that any standing water body was relatively shallow, possibly seasonal and bioturbated (Jones, 2010). Artefacts are absent from Locality 3 during this phase, with occupation pushed towards the valley margins and the edge of the floodplain area (Haslam, 2008). Sediment organic content remains below 2% through Phases 1 and 2, which demonstrates that organic turnover was high through this period. This period coincides in part with the high sedimentation seen in Arabian Sea cores (Schultz et al., 2002; Von Rad et al., 2002) for the initial climatic deterioration from the peak of Dansgaard–Oeschger (D–O) interstadial 20, dated approximately 77 ka in the North Greenland ice core (Andersen et al., 2004) and 73 ka in the Greenland Summit ice record (Dansgaard et al., 1993). The soil carbonate oxygen isotope record for Locality 3 through Phases 1–3 reveals a distinct cooling/drying trend throughout the period leading to the Toba eruption (Fig. 6). Interestingly, while the steady ^{18}O enrichment of Locality 3 parallels the development of more open environments documented by the ^{13}C record at the site, the sedimentary sequence for Phases 1–3 suggests that local fluvial hydrology, and potentially therefore monsoon rainfall patterns, remained variable.

The fourth depositional phase (Phase 4, Stratum C) at Locality 3 is formed by horizontally-bedded Youngest Toba Tephra layers. Initial deposition is seen in a ~4 cm layer, interpreted as a record of primary ash-fall tephra, and subsequent build-up of redeposited material appears to have followed a cyclical wet-dry process resulting in a maximum thickness of some 2.4 m of relatively pure Toba tephra at Locality 3. While the primary tephra most likely settled directly into a still water environment, it is likely that the

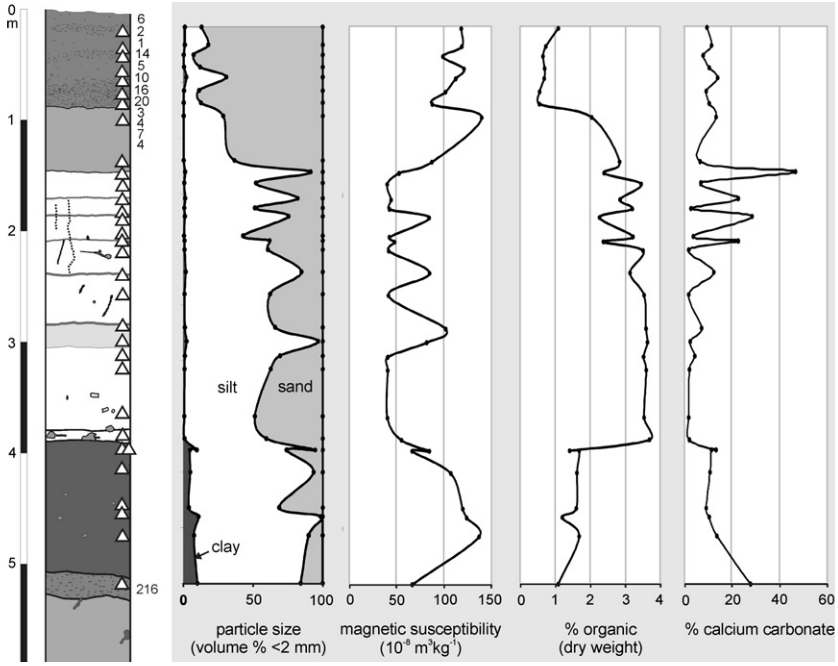

Fig. 5. Particle size, magnetic susceptibility, organic loss on ignition and calcium carbonate percentage data for Jwalapuram Locality 3 (after Jones, 2010). Triangles indicate sediment sample locations, numbers beside the profile indicate artefact counts.

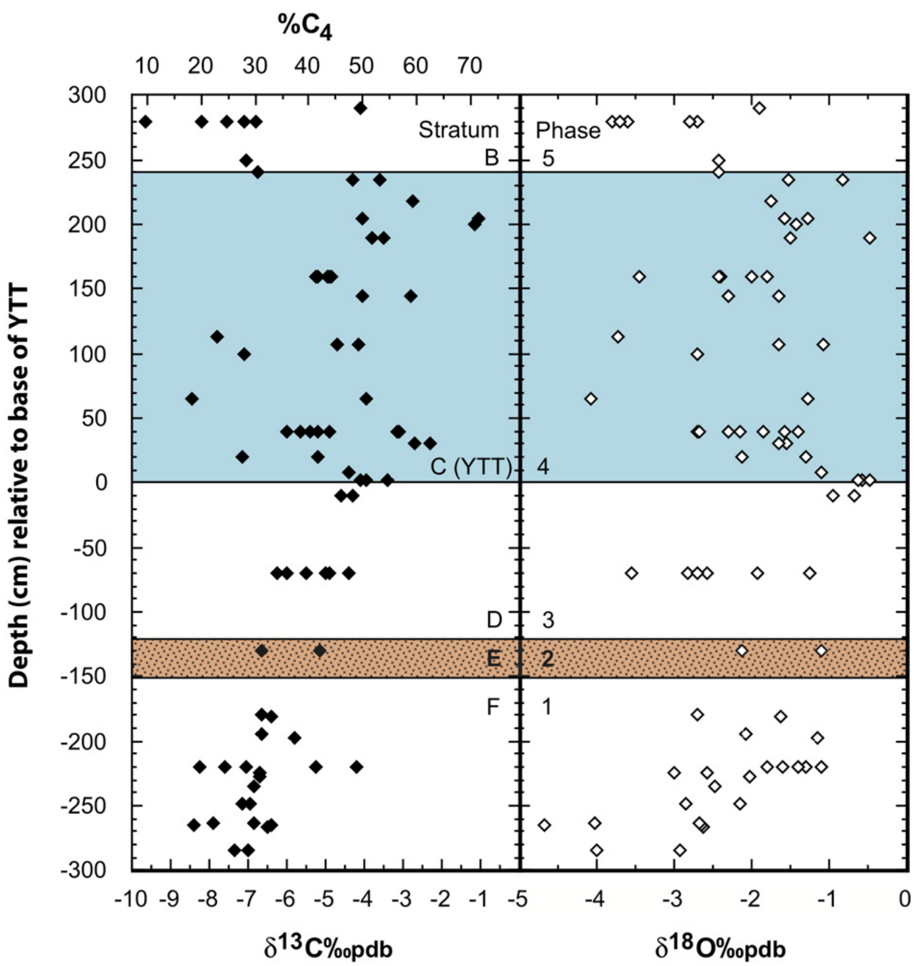

Fig. 6. Carbon and oxygen isotope records, Jwalapuram Locality 3 (negative depth values represent samples collected beneath the YTT deposit; for details of sedimentary phases see text).

overlying redeposited sediments were subject to aeolian and possibly colluvial transport within a relatively short timeframe. A recent unpublished mapping project conducted in the Jurreru Valley as part of KDAP demonstrates that Locality 3 was a significant local topographical low and therefore a sediment trap. After the eruption, when unconsolidated tephra likely formed the primary surface sediments across southern India, aeolian transport and potentially slope-wash appear to have shifted quantities of ash into standing water without significant influx of other detritus. Each of the six distinct beds within the tephra (with the primary fall forming the basal component of the lowest bed) follow a similar pattern of upward fining sediments, capped by a continuous hardpan exhibiting mudcracking and fossil plant remains. These episodes are interpreted as aerial exposure of the settled ash during seasonal dry periods, followed by the re-expansion of the palaeowetlands (again without a significant non-tephra sediment load) and further YTT accumulation into standing water conditions. It is possible that the continued presence of YTT across the landscape contributed to the repeated re-establishment of the ash-choked water body, with annual monsoons driving the cycle over a ~6 year period. Phase 4 sedimentology records high magnetic susceptibility and calcium carbonate levels for the hardpan layers, with the latter increasing up the profile. The less dense tephra layers have low susceptibility and carbonate contents, and preserve the highest organic content of any sediments at the site. The organic content may in part derive from flooding events, as in places the YTT deposits encapsulate both standing and fallen trees.

The isotopic record at the site shows a variable signal of both ^{13}C and ^{18}O throughout the period of YTT ash deposition. However, an overall increasing trend in values is apparent in the top 100 cm of Stratum C, reflecting 50–70% C_4 biomass, equivalent to a more open wooded grassland. It is likely that the Toba ash had an at least initially significant detrimental effect on local vegetation, with grasslands re-establishing themselves during the final stages of ash clearance from topographical highs in the surrounding area. Two phases follow the YTT accumulation at Jwalapuram Locality 3. Phase 5 (Stratum B) sediments comprise ~60 cm of orange silty sand with a decreasing ash content moving up the profile, aligned to increasing magnetic susceptibility and decreasing organic content. This marks the first phase since the Toba eruption with significant non-tephra sediment input into the site, which combined with the increased magnetic susceptibility may indicate that the landscape was stabilising throughout this period. The area was inhabited by Middle Palaeolithic hominins in the latter stages of Phase 5 (Fig. 5), and the lack of artefacts immediately following landscape stabilisation may be the result of occupational hiatus at this particular location in the valley. Carbon and oxygen isotope ratios resemble those at the base of Stratum F, with 25–35% C_4 plant biomass, indicating a return to grassy woodlands.

The final phase of sediment accumulation at Locality 3 (Phase 6, Stratum A) saw continuous artefact accumulation. Sediments are variable throughout this period with an ~80 cm build-up of lenses of pebbles and sands interspersed among orange silts. While a portion of this material may result from minor channel formation it is likely that the majority was deposited by surface run-off and localised flooding events. These indicate a return to wetter conditions in the Jurreru Valley. Wet conditions also would have contributed to artefact movement at the site, however artefacts are the only large clasts in the Phase 6 sediments, indicating typically lower energy events and that redeposition would have been minor. In Trenches 3B and 23 this stratum contains small, discrete pods of relatively pure Toba ash indicating that during this period earlier Phase 4 deposits were occasionally exposed and entrained for short distances. Sediments in Phase 6 show occasional cross-bedding, and we propose that this phase is linked to the formation of a series of low terraces created by the northwards migration of the Jurreru River during the Late Pleistocene. Fluctuating magnetic susceptibility during this phase supports this assessment. The upper portion of this stratum returned an OSL age of 74 ± 7 ka (JLP-380; Petraglia et al., 2007) from multi-grain aliquots, and single-grain OSL analysis of the same sediments is planned to assess any potential effects of sediment mixing (Arnold and Roberts, 2009; Jacobs and Roberts, 2007). Note that the sediments at Jwalapuram Locality 3 have only a thin cap of modern soil development following Phase 6 deposition (stratum A), likely as a result of cessation of sediment aggradation at this site as the river moved away, combined with minor erosion of the exposed upper surface of the now-infilled topographical low.

Phytolith analyses (Eksambekar, 2008) from Trench 23 provide an additional perspective on the Locality 3 palaeoenvironment for Phases 5 and 6, as well as the conclusion of Phase 4. This work is in progress, with one sample analysed from each stratum so far, and results remain indicative rather than conclusive. Phase 4 phytoliths were extracted from the top of the final YTT bed, and were well preserved and mostly transparent. The average maximum phytolith size ranged above 100 microns, with a high frequency of elongate (>30% of the assemblage) and trichome morphotypes representing the Poaceae (grasses). Some representative phytoliths of the Acanthaceae and Burseraceae/Fabaceae families are also present, with the tentative conclusion that this assemblage likely derives from wind transport from surrounding open grassland areas. Phase 5 phytoliths were smaller on average and showed slight occlusion. Grass families continue to be important (although elongate morphotypes drop to low levels), with a corresponding increase in representatives of the Amaranthaceae, Acanthaceae and Burseraceae/Fabaceae families. This composition is on the whole similar for the final Phase 6, however in the latter it is accompanied by a tripling of woody elements up to 9% of the total assemblage and an additional increase in spherical (possibly Amaranthaceae) morphotypes. These initial results concur with the isotopic data in suggesting an open and possibly wooded grassland environment in the Jurreru Valley after the Toba event, with a more significant woodland element emerging in the wetter Phase 6.

4. Lithic technology before and after the Toba eruption

Table 3 presents data on the number of artefacts recovered from each trench within Locality 3, all of which were subjected to the same detailed technological attribute analysis and classification. The measured attributes and recording techniques are described in detail elsewhere (Clarkson, 2007; Petraglia et al., 2009a, 2007). Fieldwork over the past three years has increased lithic sample sizes both below and above the Toba ash at Locality 3 by more than 50%, providing greater insight into the activities represented at the site. Representative artefacts are illustrated in Fig. 7.

4.1. Lithic technology at Locality 3

There are essentially no differences between artefacts from strata A and B above the ash layer, and these have therefore been combined to create the above ash sample, with the below ash sample derived from stratum E in trench 3A. Comparisons of assemblage composition above and below the ash at Locality 3 show very few differences (Table 4). Most typological differences are in the order of less than 1% of the assemblage, with the most varied categories including flakes, flaked pieces, notches, side scrapers and multiplatform cores. Differences in the proportions of flakes and flaked pieces may reflect fragmentation rather than real technological differences. The higher proportion of flaked pieces

Table 3
Artefact classification by trench, Jwalapuram Locality 3.

	Trench				
	23	3	3A	3B	Total
Blade		3	6		9
Burin		1			1
Burin Spall		1			1
Burinated Scraper			1		1
Core Fragment	1	2	1		4
Double Side and End Scraper		1	4		5
Double Side Scraper		1			1
Double Side Scraper on Blade		1			1
End Scraper		3	3		6
End Scraper on Break	1				1
Flake	24	62	258	14	358
Flaked Piece	6	17	24	6	53
Hammerstone			4		4
Levallois Core				1	1
Levallois Point			2		2
Manuport			1		1
Microblade	3		2		5
Multiplatform Core		7	3	1	11
Notched Redirecting Flake			1		1
Notched Scraper		2		1	3
Notched Side Scraper	1				1
Ochre			1		1
Ochre Crayon			1		1
Pointed Blade		2	1		3
Pseudo Levellois Point			4		4
Quartz crystal	1				1
Redirecting Flake	2		4		6
Retouched Flaked Piece		1			1
Retouched Heat Spall		1			1
Retouched Tabular Piece			2		2
Side and End Scraper	1	1	3		5
Side Scraper	3		11		14
Single Platform Core		2			2
Total	43	108	337	23	511

above the ash is consistent with a doubling of the proportion of broken artefacts, up from 17% to 30%.

Core reduction strategies show strong continuities pre- and post-74 ka, with prepared radial cores and multiplatform cores present above and below the ash. A single platform core is also found above the ash. Complete retouched and unretouched limestone flakes from above and below the ash show no significant differences in 20 variables measuring size, shape or retouch intensity and type (Table 5), reflecting the lack of change in core reduction strategies. While side scrapers are more frequent below the ash and notches more frequent above, retouched flakes show no significant differences in reduction intensity, perimeter of retouch or edge angle, nor in the number of notches present on flakes.

Levallois flakes and points are slightly more common below the ash, and a core fragment found beneath the ash at Locality 3 shows either discoidal or Levallois reduction. There is a shift in emphasis from prepared radial cores below the ash to multiplatform cores above. This shift is also reflected in flake dorsal scar patterns (Fig. 8), with a reduction in radial scar patterns and an increase in non-proximal scar patterns (i.e. from left, right, distal or combinations of these) indicative of removal from rotated cores with platforms orientated in various ways. Bidirectional scar patterns could result from either radial or multiplatform cores, and show little proportional difference above and below the ash. Platform faceting also reduces in frequency after Toba (from 9.6 to 2.9%), consistent with less concern for preparing platforms for large removals with forceful blows and increased concern for striking multiple flakes from the same edge.

Raw materials (Table 6) show an increase in the proportion of limestone relative to total weight of stone above the ash, along with

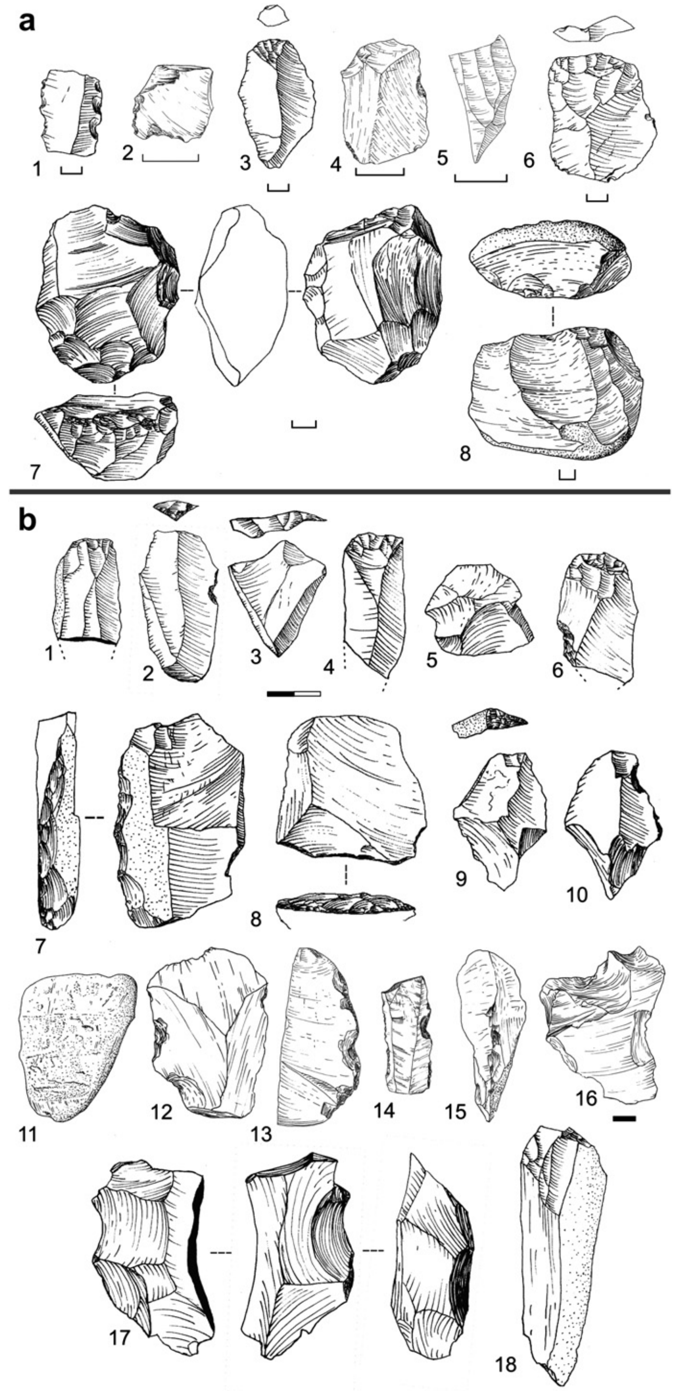

Fig. 7. Lithic artefacts recovered from Jwalapuram Locality 3: (a) *Above YTT*: 1, broken retouched blade (Trench 3B); 2 and 4, lightly retouched/utilised flake (Trench 3); 3 and 6, flake (Trench 3B); 5, broken blade (Trench 3); 7, opposed recurrent Levallois core (Trench 3B); 8, flake core with faceted platform (Trench 3). (b) *Below YTT*, all artefacts from Trench 3A: 1, 7, 12 and 13, side retouched flake; 2, Levallois blade; 3, pseudo-Levallois point; 4, broken blade; 5, Levallois flake; 6 and 14, side retouched broken blade; 8, end retouched flake; 9, pseudo-Levallois flake; 10, notch; 11, ochre; 15, lightly retouched ridge straightening flake; 16, double side and end retouched flake; 17, radial core fragment; 18, large elongate flake. Scales in cm.

a slight increase in mean artefact weight (excluding cores), whereas quartzite reduces dramatically in proportion of total weight and dolerite drops out entirely. Chert, chalcedony and crystal quartz are present in roughly equal proportions of total weight of stone above and below the ash, but show a reduction in average artefact weight.

Table 4
Percentage difference in artefact types below and above ash, Jwalapuram Locality 3 (positive difference values indicate higher prevalence above the ash).

	Above	Below	Total	Above %	Below %	Difference
Flaked Piece	29	24	53	16.48	7.12	9.36
Multiplatform Core	8	3	11	4.55	0.89	3.66
Notched Scraper	3		3	1.7	0	1.7
Core Fragment	3	1	4	1.7	0.3	1.41
Single Platform Core	2		2	1.14	0	1.14
Microblade	3	2	5	1.7	0.59	1.11
Pointed Blade	2	1	3	1.14	0.3	0.84
End Scraper	3	3	6	1.7	0.89	0.81
Burin	1		1	0.57	0	0.57
Burin Spall	1		1	0.57	0	0.57
Double Side Scraper	1		1	0.57	0	0.57
Double Side Scraper on Blade	1		1	0.57	0	0.57
End Scraper on Break	1		1	0.57	0	0.57
Levallois Core	1		1	0.57	0	0.57
Notched Side Scraper	1		1	0.57	0	0.57
Quartz crystal	1		1	0.57	0	0.57
Retouched Flaked Piece	1		1	0.57	0	0.57
Retouched Heat Spall	1		1	0.57	0	0.57
Side and End Scraper	2	3	5	1.14	0.89	0.25
Redirecting Flake	2	4	6	1.14	1.19	−0.05
Blade	3	6	9	1.7	1.78	−0.08
Burinated Scraper		1	1	0	0.3	−0.3
Manuport		1	1	0	0.3	−0.3
Notched Redirecting Flake		1	1	0	0.3	−0.3
Ochre		1	1	0	0.3	−0.3
Ochre Crayon		1	1	0	0.3	−0.3
Levallois Point		2	2	0	0.59	−0.59
Retouched Tabular Piece		2	2	0	0.59	−0.59
Double Side and End Scraper	1	4	5	0.57	1.19	−0.62
Hammerstone		4	4	0	1.19	−1.19
Pseudo-Levallois Point		4	4	0	1.19	−1.19
Side Scraper	3	11	14	1.7	3.26	−1.56
Flake	100	258	358	56.82	76.56	−19.74
Total	174	337	511			

Quartz and quartzite also show a reduction in average artefact weight. Limestone is the dominant raw material both above and below the ash. The combined data suggest more extensive reduction of higher-quality materials (cherts and chalcedony) above the YTT, however core sample sizes do not currently permit further assessment of this notion.

Table 5
Significance of differences in recorded values for complete limestone flakes above and below ash, Jwalapuram Locality 3.

	t	df	Sig. (2-tailed)	Mean difference[a]
Weight	1.26	153	0.210	8.04
Length	−0.11	33	0.910	−0.55
Proximal Width	−0.73	42	0.467	−1.63
Medial Width	−0.89	32	0.381	−3.03
Distal Width	−0.68	150	0.500	−1.43
Maximum Dimension	−0.34	70	0.736	−1.68
Thickness	−1.13	40	0.263	−1.46
Maximum Width	−0.42	41	0.678	−1.49
Platform Width	−0.20	145	0.840	−0.51
Platform Thickness	−0.08	147	0.939	−0.09
Platform Angle	1.24	148	0.216	3.64
Dorsal Scar Count	−1.00	63	0.323	−0.37
Number of Retouched Segments	0.00	8	1.000	0.00
% Cortex	−0.77	149	0.440	−4.89
Elongation (Length:Width)	0.84	150	0.404	0.12
Average GIUR[b]	−0.33	153	0.739	−0.01
Average Retouch Angle	−0.11	153	0.913	−0.31
Retouch Curvature	0.93	8	0.379	0.27
% Edge Retouched	0.76	8	0.468	0.16
Length:Thickness	0.53	152	0.600	0.22

[a] Positive means represent higher values for artefacts above the ash, negative means represent higher values for artefacts below the ash.
[b] GIUR: Geometrical Index of Unifacial Reduction (Kuhn, 1990).

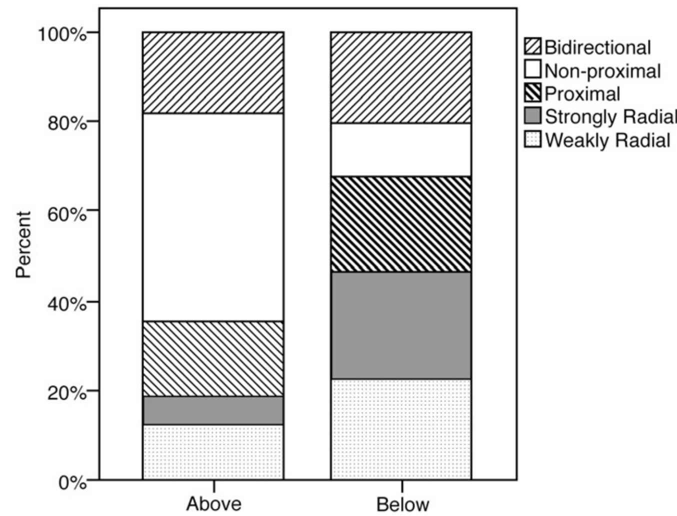

Fig. 8. Flake dorsal scar patterns from above and below YTT deposits, Jwalapuram Locality 3.

4.2. Who made the pre- and post-YTT assemblages?

Previously it has been hypothesised that *H. sapiens* groups occupied Locality 3 both prior and subsequent to the YTT event (Petraglia et al., 2007). If this was the case, then we can expect the technological strategies at the site to show closer affinities to African centres of potential human dispersal than to other unrelated regional lithic assemblages. Initial results using discriminant analysis based on core shape and technology suggested that this was indeed the case (Petraglia et al., 2007), and for this study we have used an expanded dataset to compare core reduction strategies from Middle Stone Age and Middle Palaeolithic sites in Africa, Europe and the Levant to further test this hypothesis.

Our discriminant analysis employed 827 cores from 30 sites (Table 7), using methods described in Petraglia et al. (2007:SOM). Fig. 9 presents the discriminant analysis results, with Functions 1 and 2 together accounting for 93.8% of the variation ($F1 = 50.9\%$, $F2 = 42.9\%$), and with all functions significant at $p < 0.0005$. Five variables effectively discriminate between populations: a transformed index of the proportion of elongate flake scars on cores (0.718), an index of the height of intersection between core faces (−0.392), the number of scars on cores (−0.105), the scar pattern angle (−0.209), and the ratio of core width and thickness (axes 2 and 3) (0.665). Furthermore, individual cores classify better back into their type (52%) (e.g. discoidal, blade, single platform, multiplatform, Levallois) or regional grouping (41%), shown in Fig. 9, than they do into their raw material type (28%).

The core analysis indicates that neighbouring pre- and post-YTT assemblages cluster together with core technologies from sub-Saharan Africa. Neanderthal, Indian Late Acheulean and southwest Asian early modern human technologies are conspicuously separated from the Jurreru Valley technologies. Notably, the sample of European and southwest Asian Neanderthal technologies cluster very closely together. Middle Palaeolithic and Aterian assemblages from Libya and Morocco and are more similar to Neanderthal technologies of Europe and southwest Asia than those of southern Africa and India. This may reflect their proximity to Europe and the Levant, or it may point to the presence of different groups employing more typically Mousterian-type technologies similar to those of early *H. sapiens* in the Levant. The data also suggest that Indian Late Acheulean technologies are disjunct from the southern Indian Middle Palaeolithic, which may relate to the activities of

Table 6
Raw material exploitation above and below the ash, Jwalapuram Locality 3.

		Material[a]							
		Chal.	Chert	C. Quartz	Dolerite	Limestone	Ochre	Quartz	Quartzite
Weight (g)	Above	44.7	113.5	4.3	–	1073.4	–	12.8	76.9
	Below	127.5	442.4	–	630.4	2665.7	58.4	30.7	1241.4
% of Total Weight (g)	Above	3.24	8.22	0.31	–	77.70		0.93	5.57
	Below	2.45	8.51	–	12.13	51.30	1.12	0.59	23.89
Average Artefact Weight (g)	Above	1.54	2.64	1.08	–	16.02	–	2.56	4.81
	Below	9.81	12.64	–	78.80	12.40	19.47	15.35	21.40
% Total Artefacts	Above	1.86	4.72	0.18	–	44.65	–	0.53	3.20
	Below	0.73	2.53	–	3.60	15.22	0.33	0.18	7.09

[a] Chal. = chalcedony; C. quartz = crystal quartz.

different hominin species in the subcontinent, although further data are required to test this hypothesis. The stark contrast between assemblages of Middle Palaeolithic character and those of the early Upper Palaeolithic and microlithic does not support the notion that core technologies in southern India prior to ~35 ka are related to early blade technologies, contra Mellars (2006). The increased sample size employed in this analysis lends further support to the conclusion that artefacts deposited both prior to and after 74 ka in the Jurreru Valley are technologically more similar to a sub-Saharan African Middle Stone Age tradition than to contemporaneous European, north African or Levantine assemblages.

Table 7
Sites and core counts used in the discriminant analysis presented in Fig. 9.

Site	Frequency	%
European Neanderthals		
Combe-Capelle, France, Mousterian Layers	7	0.8
La Micoque, France, Mousterian Layers	6	0.7
Le Moustier, France, Mousterian Layers	19	2.3
SW Asian Neanderthals		
El Wad, Israel, Layers F & G	39	4.7
Skhul, Israel, Layers B–B2	36	4.4
Tabun, Israel, Layers C & D (Jelinek's 5-68)	57	6.9
Sub-Saharan Africa		
Klein Kliphuis, South Africa, Layers NGR8–16	44	5.3
Klasies River Mouth Cave 1A, South Africa, Layer 10	46	5.6
Klasies River Mouth Cave 1, South Africa, Layers 14–19	47	5.7
Melikane, Lesotho, Layers 22–24 (MSA and Howiesons Port)	53	6.4
Mumba, Tanzania, Layers V & VI	169	20.4
Diepkloof, South Africa, Howiesons Poort, pre- & post-Howeisons Poort	34	4.1
Rose Cottage Cave, South Africa, Layers EHD, EMD, ETH	36	4.4
Garoe, Somalia, 'Upper and Lower Levallois' Layers	14	1.7
Porc Epic, Ethiopia, MSA Layers	4	0.5
Eil, Somalia, Still Bay and Magosian	4	0.5
Sibudu, South Africa, Post Howiesons Poort MSA Layers	26	3.1
Gure Warbei, Somalia, Magosian Layers	5	0.6
H5, Hargeisa, Somalia, Uppers Still Bay Layers	1	0.1
Hollow Rock, South Africa, Still Bay Layers	3	0.4
Jesomma, Somalia, Magosian & Upper and Lower Levallois	4	0.5
NW African Middle Palaeolithic and Aterian		
Tabelballa, El Azrir, Morocco, Aterian	23	2.8
Haua Fteah, Libya, Layers XXVI-XXXV	59	7.1
Indian Pre-Toba		
JWP Locality 22, Kurnool District, India	17	2.1
JWP Locality 3a, Kurnool District, India	3	0.4
Indian Post-Toba		
JWP Locality 20, Kurnool District, India	5	0.6
JWP Locality 3, Kurnool District, India	5	0.6
Indian Microlithic		
JWP Locality 9, Kurnool District, India, Layers C and D	24	2.9
Eurasian Upper Palaeolithic		
Kebara, Israel, Layer E	8	1.0
Vogelherd, Germany, Layers IV and V	25	3.0
Indian Late Acheulean		
Ramnagar, Middle Son Valley, India	4	0.5
Total	827	100.0

5. Discussion

It has been hypothesised that the YTT event caused significant worldwide environmental deterioration (Rampino and Ambrose, 2000; Williams et al., 2009), including widespread destruction of both deciduous and evergreen tree taxa caused by a sharp drop in global temperatures (the use of the term 'volcanic winter' for such a drop is discussed by Dorries, 2008). If time-averaged deep sea core data are used (e.g., Ninkovich et al., 1978), the timing of the YTT eruption during the transition from OIS 5 to OIS 4 adds a potential element of confusion to any attribution of climatic effects to Toba. However, the Greenland GISP2 ice core unambiguously shows that a large sulfate pulse attributed to Toba (Zielinski et al., 1996) occurs during Dansgaard–Oeschger interstadial 20. The cold phase of D-O 20 does not mark the onset of OIS 4, which occurs after the next interstadial warm event (D-O 19), several millennia later. As demonstrated by Fig. 10, and contrary to some previous interpretations (e.g.,Williams et al., 2009:Fig. 5), neither does the YTT sulfate spike mark the initiation of an abrupt decline in temperatures that terminates the warm phase of D-O 20. Instead, ^{18}O isotopes from the GISP2 core show that this rapid decline was underway for approximately 200 years before the Toba sulfate signal appears. The YTT eruption occurs immediately prior to

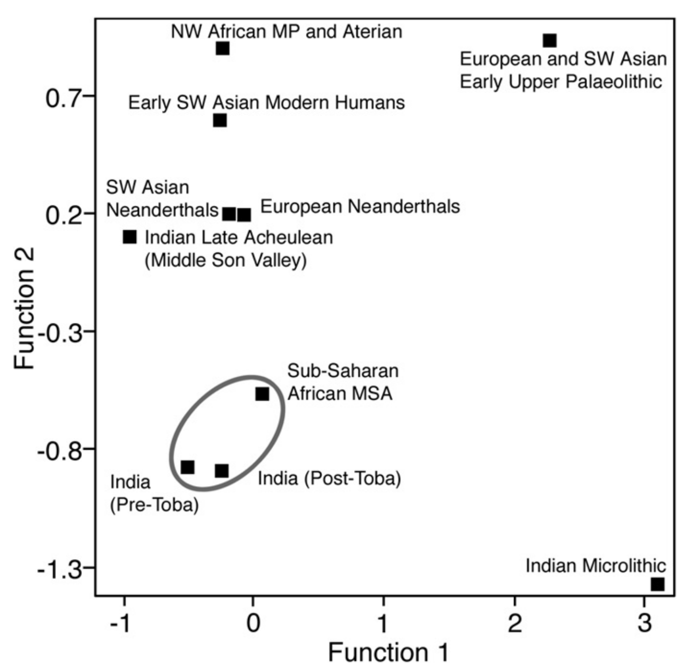

Fig. 9. Canonical discriminant function comparison of regional core reduction strategies, including the Jwalapuram data from below and above the Toba tephra, showing group centroids. Details of sites included in each data point are provided in Table 7. MSA: Middle Stone Age; MP: Middle Palaeolithic.

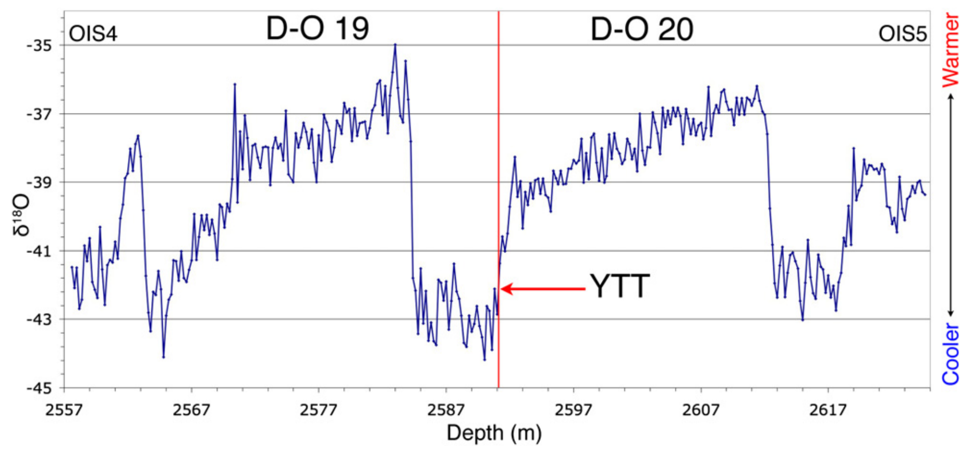

Fig. 10. High resolution (20 cm sample-spacing) oxygen isotope data from the GISP2 ice core, obtained from the University of Washington Quaternary Isotope Laboratory (http://depts.washington.edu/qil/datasets/gisp2_measured.txt). Data are from depths of 2624.6–2557.6 m (dated 75–65 ka according to the GISP2 timescale; Meese et al., 1994). The Toba-attributed sulfate spike initially occurs at a depth of 2591.12 m in the GISP2 core (Zielinski et al., 1996), marked on the figure as both a vertical line and horizontal arrow. These data demonstrate the D-O 20 cooling trend prior to the eruption, and show that Toba precedes an isotopically variable cold period prior to the inception of D-O 19.

a ~1000 year variably cold period, which has been described as the longest period with consistently low temperatures recorded in the Greenland cores (Williams et al., 2009). A similar but slightly warmer and shorter variably cold period occurred prior to D-O 20 (Fig. 10), leading Zielinski et al. (1996) to suggest that the D-20 stadial conditions would have occurred without the Toba eruption. These findings leave Toba's climatic impact on the Greenland record somewhat ambiguous (Robock et al., 2009), and proposals of a millennial-scale climatic impact of the Toba eruption (Ambrose, 1998; Rampino and Ambrose, 2000; Williams et al., 2009) remain open to question.

Recent computer models (Robock et al., 2009) suggest that a large volcanic eruption such as Toba could negatively affect broadleaf evergreen and tropical deciduous species, and lead to an expansion of tropical grasslands. However, in all such simulations these effects last from a few months to decades at most, and wider effects such as ongoing glaciation are not triggered even under the most severe parameters (Jones et al., 2005; Robock et al., 2009). Isotopic analysis of Phase 5 paleosol carbonates from the Jurreru Valley suggest that the YTT eruption did not have an enduring environmental impact on the Kurnool region. At Jwalapuram Locality 3, prior to the YTT eruption, the isotopic data demonstrate a distinct trend towards a drier environment with increasing input from C_4 plants. This trend mirrors the overall decline in temperatures (initially gradual and then sudden) seen in the Greenland ice cores prior to YTT, following the rapid temperature rise that initiates the D-O 20 interstadial (Andersen et al., 2004; Dansgaard et al., 1993) (Fig. 10). The pre-Toba isotopic changes seen at Locality 3 therefore provide evidence that similar cooling was underway in southern India prior to the YTT event, independent of the volcano's effects. While mindful of error margins, the 77 ± 6 ka Phase 1 OSL age at Locality 3 broadly suggests a multi-millennial timespan for this cooling, which would incorporate much of D-O 20 as seen in the Greenland record. However, the direct local applicability of the high-latitude climate record to southern India has yet to be fully resolved.

During the YTT event, and subsequently during the residence time of significant tephra redeposition in the landscape, the river channel and surrounding topographic lows were repeatedly choked by wind-borne and potentially water-borne ash. The hydrology of the valley would have been altered, but continued water input (either seasonal or perennial) is indicated by the wet-dry cycles that produced six distinct bands of tephra deposition at Jwalapuram Locality 3. Significantly, the massive accumulation of relatively pure tephra in the valley, beyond the initial ~4 cm primary ash-fall, indicates that large areas of the surrounding landscape were rapidly denuded of their ash load. If the relatively pure tephra layers at Jwalapuram Locality 3 derive from seasonal (monsoon-driven) hydrological flux, then it is likely that vegetation in the Jurreru Valley would have been able to re-establish itself within a few decades of the eruption, consistent with computer models (Robock et al., 2009). Vegetation during the tephra accumulation saw an increased grass component, as indicated by phytolith analysis and a continued increase in the C_4 isotopic signal. This pattern is similar to that reported at YTT-bearing sites in north-central India (Williams et al., 2009), where wooded grasslands to grasslands persisted for varying amounts of time after the eruption deposited ash onto an initially forested landscape. However, in the Jurreru Valley the particular depositional circumstances and short timespan (likely at most decadal) represented by Phase 4 YTT deposits means that the grass signature seen at the top of this phase cannot be used as evidence of Toba's impact on any geographic scale other than the local. Furthermore, the pattern of increased grass indicators within the tephra layer in both the northern and southern sites is to be expected given the tendency for grasses to act as initial colonisers of an ashy substrate, and should not *a priori* be read as a record of climate-driven grassland development (Fuller and del Moral, 2003; Halpern et al., 1990; Lentfer and Boyd, 2001; Lentfer and Torrence, 2007; Whittaker et al., 1989). Variable carbon isotope values from within the tephra may partially derive from the more wooded slopes of the Jurreru Valley surviving the initial fall and rapidly losing their ash load, or from colonising C_3 forbs and grasses, however overall a wooded grassland signal remains during this period. Comparing this signal with the heavily forested environment seen before and after the Toba eruption in portions of the north Indian Narmada and Middle Son Valleys (Williams et al., 2009) supports vegetation reconstructions of a mosaic palaeoenvironment across South Asia in late OIS 5 (Petraglia et al., 2010).

Hominins in the Jurreru Valley prior to the Toba eruption inhabited grassy woodlands, with a shift towards wooded grasslands at the time of the initial ash influx. Extensive systematic survey of the Jurreru Valley and surrounding areas indicates that Middle Palaeolithic occupation was concentrated close to raw material sources exclusively on the broad valley floor (Shipton et al., in press). This settlement pattern would have brought hominins into close contact with large herbivore taxa drawn to the mosaic riverine habitat, but also would have required an increase in mobility following the YTT ash-fall, as groups relocated to areas closer to freshwater outlets in the surrounding upland areas or moved out of the valley altogether. Aquifer-fed springs are located in the surrounding sandstone plateaus, and the combination of cleared areas and freshwater sources would have offered resident hominins and other fauna and flora the opportunity to persist in the general area even as tephra built-up in the Jurreru itself. Ambrose (1998) notes that southern India would have acted as a biotic population refugium during any 'volcanic winter' associated with Toba, although he notes that ash coverage may have diminished its potential. With much of the area to the west, south and north of Jwalapuram Locality 3 consisting of higher terrain likely to have quickly shed its ash cover (Fig. 1), local extinction of hominin populations is unlikely to have occurred from a lack of water or complete loss of prey species habitat. Over-exposure to wind-borne tephra particles can have negative health consequences (Horwell and Baxter, 2006), however the effects are typically cumulative. The example of local Jwalapuram villagers quarrying and sieving YTT for several hours each day over several years, without protective equipment, demonstrates that the hazards of even prolonged exposure do not manifest sufficiently rapidly to lead to widespread fatalities.

Following the stabilisation of the major ash beds the river may have been further south (closer to Jwalapuram Locality 3) than at present, as suggested by the silty sand soil that developed on top of the YTT deposits. The occupational hiatus seen at the site suggests that this particular part of the valley was less suitable for habitation than the surrounding areas while the grassy ash surface was dominant. However, re-occupation of the valley bottomlands took place while the Phase 5 soil was still accumulating. The establishment of sandy riverbanks and gravel beds, along with an abrupt decrease in oxygen isotope values and a return to grassy woodland signatures in both the carbon isotope and phytolith records, indicates that rainfall continued during the post-74 ka period represented by the Locality 3 sediments. This environment likely attracted not only hominin groups but other animal taxa following water sources and browsing opportunities. It is significant that this re-occupation occurred even in a locality that would have experienced regular re-exposure of YTT deposits and their aeolian and fluvial entrainment, as spring sites away from the central Jurreru bottomlands should have been even more attractive.

Explanations for the re-occupation of Locality 3 can be assessed against the lithic data that show few significant changes before and after 74 ka. The accompanying wet and likely wooded signals derived from the sediment and palaeoenvironment indicators suggest the return of hominins during favourable conditions, after an initial hiatus. Technological strategies employed by the hominin groups demonstrate continuity within a Middle Palaeolithic tradition, with an increased emphasis on smaller artefacts made from high-quality raw materials. This shift may result from slight cultural drift in flaking traditions over time. There is no evidence that the post-74 ka populations were technologically disjunct from earlier groups at Locality 3, with continuation of Middle Palaeolithic traditions dominated by local limestone in the Jurreru valley until at least 38 ka (Petraglia et al., 2009a). Neither is there any evidence that the Locality 3 occupants possessed a systematic microlithic technology. The technological similarities below and above the Toba isochron suggest that the post-74 ka occupation at Locality 3 was by indigenous groups, and not newly arrived colonists from Africa or elsewhere carrying new technologies. In this view, Indian human populations were probably not driven to extinction by Toba.

Regional comparison of core reduction strategies indicates a close correlation between Middle Stone Age assemblages from sub-Saharan Africa and the Jurreru Valley assemblage both above and below the Toba tephra. While a large region, sub-Saharan Africa is also suggested by genetic studies to be the putative origin for modern human dispersal during the Late Pleistocene (Tishkoff et al., 2009). On this basis, we cannot rule out *H. sapiens* as the creator of the Jwalapuram Middle Palaeolithic assemblage, and in fact the core comparison suggests *H. sapiens* as the most likely occupant of Locality 3. Early *H. sapiens* technology from the Levant is dissimilar to the southern Indian assemblage, raising the possibility that anatomically modern humans followed more than one route out of Africa during OIS 5, with loss of genetic lineages between then and now. Consideration of recent archaeological evidence from Arabia and South Asia lends further support to the notion of a Middle Stone Age/Middle Palaeolithic *H. sapiens* dispersal out of Africa during OIS 5 (Petraglia et al., 2010), contrary to a hypothesised OIS 4 dispersal accompanied by microlithic artefacts (Mellars, 2006). Instead, systematic microlithic technologies appear in South Asia (including the Jurreru Valley) by around 35 ka, corresponding to a marked demographic expansion within the subcontinent and signalling this as an autochthonous development (Clarkson et al., 2009; Petraglia et al., 2009a).

6. Conclusion

To conclusively determine the maker(s) of South Asian Late Pleistocene lithic assemblages, there remains a pressing need for recovery of hominin skeletal material dating to OIS 5 and OIS 4. In its absence, however, quantitative analyses of lithic technological strategies in the Jurreru Valley, accompanied by palaeoenvironmental reconstruction and chronometric dates, provide the highest resolution data currently available for hominin activities in India. Hominins using core reduction strategies technologically very similar to those of Middle Stone Age Africa appear to have been able to take advantage of the return to climatically favourable conditions after the undoubtedly dramatic short-term impact of the YTT ash-fall and accompanying reduction in biomass across India. We propose that the populations in southern India at this time were *H. sapiens*, who continued to utilise Middle Palaeolithic techniques for the subsequent ~40,000 years in this region before indigenous demographic changes prompted and responded to a shift to microlithic technology. We have demonstrated that an environmental shift towards drier, cooler conditions was underway well before the YTT ash-fall in southern India, which would have resulted in changes in resource availability and mobility patterns among southern Indian hominins even prior to the sudden and short-lived effects of Toba. In any case, even in an area as heavily affected by tephra accumulation as the Jurreru Valley, wooded environments were eventually re-established, accompanied by hominin re-occupation of the valley. In this regard, the mobility and flexibility of small hunter-gatherer groups in India would have provided a distinct advantage in coping with the negative consequences of the Toba super-eruption, when compared to the significant disruption to agriculture and infrastructure that modern populations faced with the same eruption today would experience (Self, 2006).

Jwalapuram Locality 3 is presently the only site in South Asia with a detailed archaeological record from both prior and subsequent to the Toba isochron. We anticipate that a varied picture of hominin responses and adaptations across India will emerge as sites in more regions are discovered, dated and analysed. Such studies will be required to assess the broad picture we have outlined, including modern human occupation of India sometime during OIS 5, severe but temporally and biotically limited effects of the 74 ka Toba eruption, and the continuation of Middle Palaeolithic technologies related to African assemblages after the YTT event.

Acknowledgements

We thank the Archaeological Survey of India for permission to conduct the fieldwork and the American Institute of Indian Studies for logistical support. We appreciate the assistance of Nicole Boivin, the villagers of Jwalapuram, and all members of the field and analysis teams, for their support. Funding was provided by the British Academy, the Leverhulme Trust and the Australian Research Council (Grants DP0987680 and DP0770446). M.H. is supported by a Leverhulme Trust Postdoctoral Fellowship. Isotopic analysis at the University of Illinois was supported in part by National Science Foundation (USA) Instrumentation Grant SBR 98-71480.

References

Ambrose, S.H., 1998. Late Pleistocene human populations bottlenecks, volcanic winter, and differentiation of modern humans. Journal of Human Evolution 34, 623–651.

Andersen, K.K., Azuma, N., Barnola, J.-M., Bigler, M., Biscaye, P., Caillon, N., Chappellaz, J., Clausen, H.B., Dahl-Jensen, D., Fischer, H., Fluckiger, J., Fritzsche, D., Fujii, Y., Goto-Azuma, K., Gronvold, K., Gundestrup, N., Hansson, M., Huber, C., Hvidberg, C., Johnsen, S., Jonsell, U., Jouzel, J., Kipfstuhl, S., Landais, A., Leuenberger, M., Lorrain, R., Masson-Delmotte, V., Miller, H., Motoyama, H., Narita, H., Popp, T., Rasmussen, S., Raynaud, D., Rothlisberger, R., Ruth, U., Samyn, D., Schwander, J., Shoji, H., Siggard-Andersen, M.-L., Steffensen, J., Stocker, T., Sveinbjornsdottir, A., Svensson, A., Takata, M., Tison, J.-L., Thorsteinsson, T., Watanabe, O., Wilhelms, F., White, J.W.C., 2004. High-resolution record of northern hemisphere climate extending into the last interglacial period. Nature 431, 147–151.

Arnold, L., Roberts, R.G., 2009. Stochastic modelling of multi-grain equivalent dose (De) distributions: implications for OSL dating of sediment mixtures. Quaternary Geochronology 4, 204–230.

Cerling, T.E., Thiry, M., Simon-Coinçon, R., 1999. Stable carbon isotopes in paleosol carbonates. In: Palaeoweathering, Palaeosurfaces, and Related Continental Deposits. Blackwell Science, Oxford, pp. 43–60.

Clarkson, C., 2007. Lithics in the Land of the Lightning Brothers: The Archaeology of Wardaman Country, Northern Territory. ANU E Press, Canberra.

Clarkson, C., Petraglia, M., Korisettar, R., Haslam, M., Boivin, N., Crowther, A., Ditchfield, P., Fuller, D., Miracle, P., Harris, C., Connell, K., James, H., Koshy, J., 2009. The oldest and longest enduring microlithic sequence in India: 35 000 years of modern human occupation and change at the Jwalapuram Locality 9 rockshelter. Antiquity 83, 326–348.

Dansgaard, W., Johnsen, S., Clausen, H., Dahl-Jensen, D., Gundestrup, N., Hammer, C., Hvidberg, C., Steffensen, J., Sveinbjornsdottir, A., Jouzel, J., Bond, G., 1993. Evidence for general instability of past climate from a 250-kyr ice record. Nature 364, 218–220.

Dorries, M., 2008. The 'winter' analogy fallacy: from superbombs to supervolcanoes. History of Meteorology 4, 41–56.

Eksambekar, S., 2008. Report of Phytolith Analysis. Submitted to R. Korisettar. Karnatak University, Dharwad (Phytolith Research Institute, Pune).

Fuller, R.N., del Moral, R., 2003. The role of refugia and dispersal in primary succession on Mount St. Helens, Washington. Journal of Vegetation Science 14, 637–644.

Halpern, C., Frenzen, P., Means, J., Franklin, T., 1990. Plant succession in areas of scorched and blown-down forest after the 1980 eruption of Mount St. Helens, Washington. Journal of Vegetation Science 1, 181–194.

Haslam, M., 1 November 2008. Recent Palaeolithic Research in the Kurnool District, Southern India. Poster Presented at the 'Major Issues on the Origins and Evolution of Modern Humans in India' Symposium, Leverhulme Centre for Human Evolutionary Studies. University of Cambridge.

Haslam, M., Korisettar, R., Petraglia, M., Smith, T., Shipton, C., Ditchfield, P., 2010. In Foote's steps: the history, significance and recent archaeological investigation of the Billa Surgam caves in southern India. South Asian Studies 26, 1–19.

Horwell, C.J., Baxter, P.J., 2006. The respiratory health hazards of volcanic ash: a review for volcanic risk mitigation. Bulletin of Volcanology 69, 1–24.

Jacobs, Z., Roberts, R.G., 2007. Advances in optically stimulated luminescence dating of individual grains of quartz from archeological deposits. Evolutionary Anthropology 16, 210–223.

Jones, G., Gregory, J., Stott, P., Tett, S., Thorpe, R., 2005. An AOGCM simulation of the climate response to a volcanic super-eruption. Climate Dynamics 25, 725–738.

Jones, S., 2007. A Human Catastrophe? The impact of the ˜74,000 year-old Super-volcanic Eruption of Toba on Hominin Populations in India. Unpublished PhD thesis, University of Cambridge, Cambridge.

Jones, S., 2010. Palaeoenvironmental response to the ~74 ka Toba ash-fall in the Jurreru and Middle Son valleys in southern and north-central India. Quaternary Research 73, 336–350.

Kuhn, S., 1990. A geometric index of reduction for unifacial stone tools. Journal of Archaeological Science 17, 583–593.

Lentfer, C., Boyd, W., 2001. Maunten Paia: Volcanoes, People and Environment. Southern Cross University Press, Lismore.

Lentfer, C., Torrence, R., 2007. Holocene volcanic activity, vegetation succession, and ancient human land use: unraveling the interactions on Garua Island, Papua New Guinea. Review of Palaeobotany and Palynology 143, 83–105.

Levin, N.F., Quade, J., Simpson, S.W., Semaw, S., Rogers, M., 2004. Isotopic evidence for Plio-Pleistocene environmental change at Gona, Ethiopia. Earth and Planetary Science Letters 219, 93–110.

Macaulay, V., Hill, C., Achilli, A., Rengo, C., Clarke, D., Scozzari, R., Cruciani, F., Taha, A., Shaari, N.K., Raja, J.M., Ismail, P., Zainuddin, Z., Goodwin, W., Bulbeck, D., Bandelt, H.-J., Oppenheimer, S., Torroni, A., Richards, M., 2005. Single, rapid coastal settlement of Asia revealed by analysis of complete mitochondrial genomes. Science 308, 1034–1036.

Mellars, P., 2006. Going East: new genetic and archaeological perspectives on the modern human colonization of Eurasia. Science 313, 796–800.

Meese, D.A., Alley, R.B., Flacco, R.J., Germani, M.S., Gow, A.J., Grootes, P.M., Illing, M., Mayewski, P.A., Morrison, M.C., Ram, M., Taylor, K., Yang, Q., Zielinski, G.A., 1994. Preliminary Depth–Age Scale of the GISP2 Ice Core Special CRREL Report 94–1.

Ninkovich, D., Shackleton, N.J., Abdel-Monem, A.A., Obradovich, J.D., Izett, G., 1978. K-Ar age of the late Pleistocene eruption of Toba, north Sumatra. Nature 276, 574–577.

Oppenheimer, C., 2002. Limited global change due to the largest known Quaternary eruption, Toba 74 kyr BP? Quaternary Science Reviews 21, 1593–1609.

Oppenheimer, S., 2009. The great arc of dispersal of modern humans: Africa to Australia. Quaternary International 202, 2–13.

Petraglia, M., Clarkson, C., Boivin, N., Haslam, M., Korisettar, R., Chaubey, G., Ditchfield, P., Fuller, D., James, H., Jones, S., Kivisild, T., Koshy, J., Lahr, M.M., Metspalu, M., Roberts, R., Arnold, L., 2009a. Population increase and environmental deterioration correspond with microlithic innovations in South Asia ca. 35,000 years ago. Proceedings of the National Academy of Sciences 106 (30), 12261–12266.

Petraglia, M., Haslam, M., Fuller, D., Boivin, N., Clarkson, C., 2010. Out of Africa: new hypotheses and evidence for the dispersal of *Homo sapiens* along the Indian Ocean rim. Annals of Human Biology 37, 288–311.

Petraglia, M., Korisettar, R., Bai, M.K., Boivin, N., Janardhana, B., Clarkson, C., Cunningham, K., Ditchfield, P., Fuller, D., Hampson, J., Haslam, M., Jones, S., Koshy, J., Miracle, P., Oppenheimer, C., Roberts, R., White, K., 2009b. Human occupation, adaptation and behavioral change in the Pleistocene and Holocene of south India: recent investigations in the Kurnool district, Andhra Pradesh. Eurasian Prehistory 6 (1–2), 119–166.

Petraglia, M., Korisettar, R., Boivin, N., Clarkson, C., Ditchfield, P., Jones, S., Koshy, J., Lahr, M.M., Oppenheimer, C., Pyle, D., Roberts, R., Schwenninger, J.-L., Arnold, L., White, K., 2007. Middle Palaeolithic assemblages from the Indian subcontinent before and after the Toba super-eruption. Science 317, 114–116.

Prasad, K.N., 1996. Pleistocene cave fauna from peninsular India. Journal of Caves and Karst Studies 58, 30–34.

Rampino, M., Ambrose, S.H., 2000. Volcanic winter in the Garden of Eden: the Toba supereruption and the late Pleistocene human population crash. In: McCoy, F.W., Heiken, G. (Eds.), Volcanic Hazards and Disasters in Human Antiquity. Geological Society of America Special Paper, Boulder, pp. 71–82.

Rao, V., Rao, C.V.N.K., 1992. Palaeontological studies of the cave fauna of Kurnool district, Andhra Pradesh. Records of the Geological Survey of India 135, 240–241.

Robock, A., Ammann, C., Oman, L., Shindell, D., Levis, S., Stenchikov, G., 2009. Did the Toba volcanic eruption of ~74 ka B.P. produce widespread glaciation? Journal of Geophysical Research 114, D10107.

Schultz, H., Emeis, K.-C., Erlenkeuser, H., von Rad, U., Rolf, C., 2002. The Toba volcanic event and interstadial/stadial climates at the Marine Isotopic Stage 5 to 4 transition in the northern Indian Ocean. Quaternary Research 57, 22–31.

Self, S., 2006. The effects and consequences of very large explosive volcanic eruptions. Philosophical Transactions. Series A, Mathematical, Physical, and Engineering Sciences 364, 2073–2097.

Shipton, C.B.J., Koshy, J., Haslam, M., Korisettar, R., Petraglia, M. Systematic transect survey of the Jurreru Valley, Kurnool District, Andhra Pradesh. Man and Environment, in press.

Sikes, N.E., Potts, R., Behrensmeyer, A.K., 1999. Early Pleistocene habitat in Member 1 Olorgesailie based on paleosol stable isotopes. Journal of Human Evolution 37, 721–746.

Tishkoff, S., Reed, F., Friedlaender, F., Ehret, C., Ranciaro, A., Froment, A., Hirbo, J., Awomoyi, A., Bodo, J.-M., Doumbo, O., Ibrahim, M., Juma, A., Kotze, M., Lema, G., Moore, J., Mortensen, H., Nyambo, T., Omar, S., Powell, K., Pretorius, G., Smith, M., Thera, M., Wambebe, C., Weber, J., Williams, S., 2009. The genetic structure and history of Africans and African Americans. Science 324, 1035–1044.

Von Rad, U., Burgath, K.-P., Pervaz, M., Schulz, H., 2002. Discovery of the Toba Ash (c. 70 ka) in a high-resolution core recovering millennial monsoonal variability off Pakistan. In: Clift, P.D., Kroon, D., Gaedicke, C., Craig, J. (Eds.), The Tectonic and Climatic Evolution of the Arabian Sea Region. The Geological Society of London, London, pp. 445–461.

Westgate, J., Shane, P., Pearce, N., Perkins, W., Korisettar, R., Chesner, C.A., Williams, M., Acharyya, S.K., 1998. All Toba tephra occurrences across Peninsular India belong to the 75,000 yr B.P. eruption. Quaternary Research 50, 107–112.

Whittaker, R., Bush, M.B., Richards, K., 1989. Plant recolonization and vegetation succession on the Krakatau Islands, Indonesia. Ecological Monographs 59, 59–123.

Williams, M., Ambrose, S.H., van der Kaars, S., Ruehlemann, C., Chattopadhyaya, U.C., Pal, J.N., Chauhan, P., 2009. Environmental impact of the 73 ka Toba super-eruption in south Asia. Palaeogeography, Palaeoclimatology. Palaeoecology 284, 295–314.

WoldeGabriel, G., Ambrose, S.H., Barboni, D., Bonnefille, R., Bremond, L., Currie, B., DeGusta, D., Hart, W.K., Murray, A., Renne, P., Jolly-Saad, M.C., Stewart, K.M., White, T., 2009. The geological, isotopic, botanical, invertebrate, and lower vertebrate surroundings of *Ardipithecus ramidus*. Science 65, 65.e61–65.e65.

Zielinski, G.A., Mayewski, P.A., Meeker, L.D., Whitlow, S., Twickler, M., Taylor, K., 1996. Potential atmospheric impact of the Toba mega-eruption ∼71,000 years ago. Geophysical Research Letters 23, 837–840.